Research Square

Preprints are preliminary reports that have not undergone peer review.
They should not be considered conclusive, used to inform clinical practice,
or referenced by the media as validated information.

Effects of dietary phage CP1925 on intestinal health and cecal microbiota in Clostridium perfringens-challenged broilers

Chongyang Zhang
Chinese Academy of Sciences
Jiayang Li
Hunan Agricultural University
Kangle Wu
Chinese Academy of Sciences
Fang Wang
Chinese Academy of Sciences
Meizhu Xie
Hunan Agricultural University
Yulong Yin
Chinese Academy of Sciences
Kang Yao
yaokang@isa.ac.cn

Chinese Academy of Sciences

Research Article

Keywords: Clostridium perfringens, bacteriophage, necrotic enteritis, broiler chickens, intestinal health, feed additive

Posted Date: November 17th, 2026

DOI: https://doi.org/10.21203/rs.3.rs-11552329/v1

License: This work is licensed under a Creative Commons Attribution 4.0 International License.
Read Full License

Additional Declarations: No competing interests reported.

Effects of dietary phage CP1925 on intestinal health and cecal microbiota in *Clostridium perfringens*-challenged broilers

Chongyang Zhang [1,2], Jiayang Li [1,3], Kangle Wu [1,2], Fang Wang [1,2], Meizhu Xie [1,3], Yulong Yin [1], Kang Yao [1]*

1 Institute of Subtropical Agriculture, Chinese Academy of Sciences, Changsha, Hunan 410125, China

2 Chinese Academy of Sciences, Beijing, 100039, China

3 College of Animal Science and Technology, Hunan Agricultural University, Changsha 410128, China

*Corresponding author: Kang Yao, MD, PhD, Institute of Subtropical Agriculture, Chinese Academy of Sciences, No. 644, Yuanda 2nd Road, Hunan 410125, Changsha China

Tel.: +86 0731-84619706, Fax: 0731-84612685, E-mail: yaokang@isa.ac.cn

All authors' email addresses (in the order of author sequence): chongyangz7931@163.com; lijiayang0511@163.com; wukangle22@mails.ucas.ac.cn; wf980313@163.com; 19974653679@163.com; yinyulong@isa.ac.cn; yaokang@isa.ac.cn.

Abstract

Background: Necrotic enteritis (NE) caused by *Clostridium perfringens* threatens broiler health and productivity, highlighting the need for alternatives to in-feed antibiotics. This study characterized phage CP1925 and evaluated the effects of its dietary supplementation on growth performance and intestinal health in *C. perfringens*-challenged broilers. A total of 180 one-day-old broilers were assigned to six groups, with six replicate pens per group: an unchallenged control, a challenged control, three challenged groups receiving CP1925 at 10^6, 10^7, or 10^8 PFU/g feed, and an unchallenged group receiving 10^7 PFU/g feed.

Results: CP1925 had an 18,159-bp genome and exhibited lytic activity only against strain CP19 among the strains tested. The highest propagation titer was obtained at a multiplicity of infection of 10. Infectivity was maintained following exposure to pH 3–12 and temperatures up to 60 °C under the tested conditions. Compared with the challenged control, supplementation at 10^7 or 10^8 PFU/g reduced jejunal and ileal *C. perfringens* DNA loads and increased thymus indices ($P < 0.05$). In challenged broilers, phage supplementation elevated serum IgA and IgG levels and intestinal IL-10, while lowering jejunal IL-6 and TNF-α levels ($P < 0.05$). Additionally, selected intestinal morphological and tight-junction indices were improved, accompanied by reduced serum diamine oxidase and lipopolysaccharide levels. Cecal butyrate concentrations increased at 10^6 and 10^7 PFU/g, whereas microbial α-diversity did not differ among groups. *Blautia* relative abundance was highest in the unchallenged phage group. Regarding growth performance, supplementation did not significantly improve overall metrics relative to the challenged control. The unchallenged phage group showed higher average daily gain and a lower feed-to-gain ratio than the unchallenged control during days 8–21, but no significant growth differences occurred

among groups during days 22–42 or 8–42.

Conclusions: Dietary CP1925 supplementation reduced intestinal C. perfringens DNA loads and improved selected inflammatory and barrier-related indices in challenged broilers without significant growth benefits. These findings support further evaluation of CP1925 as a targeted dietary intervention against *C. perfringens*-associated intestinal injury.

Keywords: *Clostridium perfringens*; bacteriophage; necrotic enteritis; broiler chickens; intestinal health; feed additive

Background

Necrotic enteritis (NE) is an economically important intestinal disease that compromises poultry health, welfare, and productivity. Its primary etiological agent, *Clostridium perfringens*, is a Gram-positive, anaerobic bacterium widely distributed in the environment and animal gastrointestinal tracts. In susceptible broilers, proliferation of pathogenic *C. perfringens* in the small intestine can cause mucosal necrosis, ulceration, and, in severe cases, mortality [1]. NetB is a pore-forming toxin with an experimentally demonstrated role in NE pathogenesis, whereas alpha toxin is not essential for disease development in the experimental models investigated [2,3]. However, disease development depends on more than pathogen proliferation: dietary factors, coccidial infection, and interactions with the intestinal microbiota can influence susceptibility and disease outcomes [4,5]. Accordingly, evaluating an intervention against NE requires assessment of pathogen abundance alongside the associated changes in mucosal structure, barrier integrity, inflammatory responses, and the intestinal microbiota.

Concerns about antimicrobial resistance and restrictions on antibiotic growth promoters have increased interest in alternative approaches to intestinal disease control in poultry [6,7]. Lytic bacteriophages offer targeted antibacterial activity by infecting and lysing susceptible bacterial hosts [7–10]. Their efficacy nevertheless depends on phage–host compatibility, formulation, delivery, and conditions within the gastrointestinal tract [11,12]. Moreover, narrow host specificity does not necessarily imply ecological neutrality. By altering susceptible bacterial populations, phages can indirectly influence non-target bacteria and microbial metabolites through interactions within the intestinal community [13]. Phage supplementation therefore warrants evaluation not only for its antibacterial activity but also for its broader effects on host intestinal health and microbial ecology.

Previous studies support the potential of phages for controlling *C. perfringens* infections in broilers. In experimental NE models, oral administration of the INT-401 cocktail reduced mortality by 92% relative to untreated challenged birds [14], while studies of other phages have reported reductions in intestinal *C. perfringens* counts and NE-associated lesions [15,16]. Dietary phage cocktails have also improved selected growth and microbial outcomes in broilers without experimental bacterial challenge [17]. Although graded doses have been evaluated in previous studies, findings obtained with different phages, preparations, and infection conditions cannot directly establish the dose–response relationship of an individual phage. In particular, whether greater pathogen suppression is accompanied by coordinated improvements in mucosal integrity, inflammatory status, and microbial metabolism requires further investigation. An integrated assessment is important because no single biomarker captures all dimensions of intestinal health in poultry [18]. Including unchallenged supplemented birds can additionally help distinguish responses associated with experimental infection from those occurring in its absence. The relevant

question is therefore whether increasing phage exposure produces consistent benefits across these outcomes, rather than whether a higher dose simply produces a larger change in any single indicator.

The present study isolated phage CP1925 using *C. perfringens* strain CP19, characterized its biological and genomic properties, and evaluated three graded doses in challenged broilers. Supplementation began before challenge, allowing assessment of a preventive feeding strategy. We hypothesized that CP1925 supplementation would attenuate challenge-associated intestinal alterations and examined whether pathogen, host, and microbial responses varied consistently across doses. To address this question, we assessed growth performance, jejunal and ileal *C. perfringens* DNA abundance, intestinal morphology, tight-junction immunostaining, immune and inflammatory indices, cecal short-chain fatty acids, and microbiota composition. An unchallenged group receiving the medium dose was included to characterize selected responses in the absence of experimental infection. Together, these comparisons were intended to determine the extent to which changes in pathogen DNA abundance were accompanied by host intestinal benefits and microbial responses.

Methods

Isolation and purification of phages

Sewage samples were collected from a commercial chicken farm in Hunan Province, China. *Clostridium perfringens* type A, obtained from Phagelux (Nanjing) Biotechnology Co., Ltd., was used as the host bacterium for phage isolation. The sewage samples were allowed to stand at room temperature for 30 min, followed by centrifugation at 12,000 × g for 3 min. The supernatant was collected and filter-sterilized through a 0.22 μm sterile membrane to remove bacterial cells.

Subsequently, the host bacterium C. perfringens was added to the filtrate, and the mixture was incubated at 37 °C for 12 h to propagate the phage. The culture was then filtered again through a 0.22-μm membrane to obtain the phage stock solution. For phage isolation, the phage stock solution was mixed with the host bacterial culture in the logarithmic growth phase, and warm 0.6% soft TY agar (TY medium per 100 mL: 0.5 g peptone, 1.5 g tryptone, 0.5 g NaCl, and 0.5 g yeast extract) was added. The mixture was immediately poured onto solid TY agar plates and incubated anaerobically at 37 °C. On the following day, individual plaques were picked and transferred into 1 mL of SM buffer, followed by incubation at 37 °C with shaking for 2 h. The phage suspension was then subjected to repeated purification using the double-layer agar plate method for 5–6 cycles until plaques with uniform morphology and size were obtained. The purified phage was subsequently characterized. Finally, the morphology of the purified phage was examined using transmission electron microscopy (TEM).

Whole-genome sequencing of phage CP1925

Genomic DNA of the isolated phage was extracted using a phage DNA extraction kit (Norgen Biotek, Canada) according to the manufacturer's instructions. The DNA concentration was determined by agarose gel electrophoresis. The extracted DNA was sent to Shanghai Lingen Biotechnology Co., Ltd. (Shanghai, China) for whole-genome sequencing. A sequencing library was prepared upon receipt of the DNA sample. After obtaining the sequencing data, quality assessment was performed, and low-quality reads were filtered using Soapnuke software to ensure reliability for downstream analysis. Clean reads were aligned to the host genome using BWA software, and host-derived sequences were removed. High-quality reads from each sample were assembled into contigs using Megahit software. The assembled contigs were compared against the

CheckV virus database to identify viral sequences, and sequencing depth was calculated using samtools depth. Gene prediction on the contigs was performed with Prokka software, and the number and length of predicted genes were quantified. All data processing and analysis were conducted by Shanghai Lingen Biotechnology Co., Ltd. (Shanghai, China).

Host range determination

The host range of the isolated phage was evaluated against a panel of bacterial strains, including three *Clostridium perfringens* strains, two *Salmonella* strains, two *Escherichia coli* strains, and two *Enterococcus faecalis* strains. The double-layer agar plate method was used, and all tests were performed in triplicate.

Optimal multiplicity of infection (MOI) determination

The optimal multiplicity of infection (MOI) was determined following established protocols. Logarithmic-phase *C. perfringens* (2.0×10^8 CFU/mL) was mixed with the phage at MOI values of 0.01, 0.1, 1, 10, and 100 in equal volumes. Mixtures were incubated anaerobically at 37 °C for 8 h. After incubation, the cultures were centrifuged at 10,000 × g for 10 min at 4 °C. The supernatant was filtered through a 0.22-μm membrane and appropriately diluted. Phage titers were then determined using the double-layer plate method.

One-step growth curve assay

A one-step growth curve analysis was generated to characterize the lytic cycle. Logarithmic-phase host bacteria were mixed with the phage at the optimal MOI determined previously. The mixture was incubated at 37 °C for 10 min, followed by centrifugation at 8,000 × g for 5 min. The supernatant was discarded, and the pellet was resuspended in 10 mL of fluid thioglycollate medium. The suspension was then incubated anaerobically at 37 °C. Samples were

collected at various time intervals (0–180 min), filtered, and serially diluted. Phage titers at each time point were determined using the double-layer plate method. All measurements were performed in triplicate, and the average values were used to plot the one-step growth curve with time on the x-axis and phage titer on the y-axis.

pH stability assay

To assess pH stability, SM buffer was adjusted to pH 1.0–14.0 using HCl and NaOH solutions. The phage stock solution was mixed with each pH-adjusted SM buffer at a ratio of 1:9 (v/v). Mixtures were incubated in a water bath at 37 °C for 1 h or 2 h. Following incubation, phage titers were determined using the double-layer plate method. Each pH condition was tested in triplicate, and the results were averaged.

Thermal stability assay

For thermal stability assessment, 1 mL of purified phage suspension was incubated in a 1.5-mL tube using a metal bath at 50, 60, 70, and 80 °C for 1 h or 2 h. Following incubation, the samples were cooled on ice for 10 min. Aliquots (100 μL) were then diluted appropriately, and phage titers were determined using the double-layer plate method. Each temperature condition was tested in triplicate, and the results were averaged.

Animal experimental design

The animal protocol was approved by the Animal Care and Use Committee of the Institute of Subtropical Agriculture, Chinese Academy of Sciences (approval number: 20250819.183). CP1925 was propagated in log-phase *C. perfringens* cultures at the optimal MOI, and the filtered lysate was adjusted to 10^{10} PFU/mL. The stock was then diluted to 2×10^6, 2×10^7, and 2×10^8 PFU/mL and mixed with wet mash feed (1:1, v/w) to achieve final concentrations of 10^6, 10^7, and

177 10^8 PFU/g, respectively. Birds received 1 g of phage-mixed wet mash as their first feeding,
178 corresponding to daily phage exposures of 10^6, 10^7, and 10^8 PFU for the LCP, MCP, and HCP
179 groups, respectively. CNP and TCP groups received an equal volume of PBS buffer without phage.
180 A total of 180 one-day-old white-feathered broilers (45.00 ± 0.20 g) were randomly assigned to
181 six groups (n = 6 replicates; 5 birds each): CNP, TCP, LCP (10^6 PFU/g), MCP (10^7 PFU/g), HCP
182 (10^8 PFU/g), and HPP (10^7 PFU/g, no challenge). The trial consisted of a pre-feeding phase (days
183 0–7) and a formal phase (days 8–42). Phages were administered daily with the first feeding, after
184 which the remaining basal diet was provided. From days 19 to 21, birds were orally challenged
185 with C. perfringens (1 mL of 1.0×10^9 CFU/mL daily); CNP and HPP received PBS. Broilers were
186 monitored daily for clinical signs. All birds had free access to feed and water throughout the study.
187 Diets (starter, days 1–21; grower, days 22–42) met or exceeded NRC requirements and contained
188 no antimicrobials (Table 1).

189 **Data recording and sample collection**

190 On day 22, blood samples were collected from the wing vein into vacuum tubes. After
191 clotting at room temperature for 2 h, the blood samples were centrifuged at 3,000 × g for 10 min at
192 4 °C, and the serum was harvested and stored at −80 °C. Subsequently, one broiler per replicate
193 was randomly selected and euthanized by cervical dislocation. The carcasses were then dissected,
194 and the thoracic and abdominal cavities were quickly opened. The liver, spleen, thymus, and bursa
195 of Fabricius were removed and weighed, and liver samples were stored at −20 °C. Jejunal and
196 ileal tissues (approximately 1 cm in length) were immediately fixed in 4% paraformaldehyde for
197 morphological analysis. Mucosal and digesta samples from the duodenum, jejunum, and ileum, as
198 well as cecal digesta samples, were collected, snap-frozen in liquid nitrogen, and stored at −80 °C.

Fresh cecal content samples were also collected in sterile tubes, snap-frozen, and stored for microbiota and short-chain fatty acid (SCFA) analysis.

Detection of *Clostridium perfringens* load in jejunal and ileal contents

Jejunal and ileal *C. perfringens* loads were determined using quantitative real-time PCR (qPCR) as described previously [19,20]. DNA was extracted using the HeaPure Stool Genomic DNA Extraction Kit (Accurate, Changsha, China). A recombinant plasmid containing the target gene fragment was used as the standard. The primers used for *C. perfringens* identification were: forward (F): 5′--TAACCTGCCTCATAGAGT-3′-and reverse (R): 5′-TTTCACATCCCACTTAATC-3′. A standard curve was generated by plotting the cycle threshold (Ct) values against the logarithm of the target gene copy number.

Serum biochemical parameter measurement

Serum levels of total protein (TP), albumin (ALB), globulin (Glo), uric acid (UA), creatinine (CREA), alanine aminotransferase (ALT), aspartate aminotransferase (AST) were measured using an automatic biochemical analyzer (Roche, Basel, Switzerland) according to the manufacturer's instructions. Serum immunoglobulin A (IgA), immunoglobulin G (IgG), immunoglobulin M (IgM), D-lactate (D-LA), diamine oxidase (DAO), and lipopolysaccharide (LPS) were measured using commercial enzyme-linked immunosorbent assay (ELISA) kits (Jiangsu Meibiao Biotechnology Co., Ltd., Jiangsu, China) according to the manufacturer's protocols.

Intestinal inflammatory cytokine measurement

Intestinal tissues were flushed, homogenized, and centrifuged at 4 °C and 3,500 × g for 15 min. Supernatants were collected for cytokine analysis. Levels of interleukin-1β (IL-1β), interleukin-6 (IL-6), interleukin-10 (IL-10), interleukin-12 (IL-12), interferon-γ (IFN-γ), and

tumor necrosis factor-α (TNF-α) in jejunal and ileal supernatants were determined using commercial enzyme-linked immunosorbent assay (ELISA) kits (Jiangsu Meibiao Biotechnology Co., Ltd., Jiangsu, China) following the manufacturer's instructions.

Intestinal morphology analysis

Jejunal and ileal tissues (approximately 1 cm in length) were collected for morphological analysis. The tissues were fixed in 4% paraformaldehyde, dehydrated through a graded ethanol series, and embedded in paraffin. Cross-sections of the tissues were prepared and stained with hematoxylin and eosin (H&E). The stained sections were examined under a light microscope. Villus height (VH) and crypt depth (CD) were measured using image analysis software, and the VH/CD ratio was calculated.

Immunohistochemical analysis

Jejunal and ileal tissues were fixed, embedded, and sectioned at 4 μm. Following deparaffinization and rehydration, antigen retrieval was performed in citrate buffer (pH 6.0). Sections were treated with 3% hydrogen peroxide, blocked with 5% bovine serum albumin, and incubated overnight at 4 °C with primary antibodies against Occludin, Claudin-1, and ZO-1 (dilution ratio of 1:100). After incubation with an HRP-conjugated secondary antibody, staining was developed using DAB and counterstained with hematoxylin. Six non-overlapping fields per section were imaged at 20× magnification under identical acquisition settings. The average optical density (AOD) was quantified using Image-Pro Plus 6.0 as integrated optical density divided by DAB-positive staining area. Values were averaged per bird and intestinal segment prior to statistical analysis.

Cecal microbiota analysis

Cecal DNA was extracted from cecal samples using the HiPure Stool DNA Kit (DC305-08, Alfa, Guangzhou, China), and integrity was evaluated by 1% agarose gel electrophoresis. DNA purity and concentration were measured using a NanoDrop 2000 spectrophotometer (Thermo Fisher Scientific, Wilmington, USA). The V3–V4 region of bacterial 16S rRNA genes was amplified using the genomic DNA as a template, followed by purification of PCR products and sequencing on the Illumina HiSeq 2500 platform (Illumina, San Diego, USA). Data processing and bioinformatics analysis were conducted by Shanghai Lingen Biotechnology Co., Ltd., using the Lingen Bio-delivery system (delivery.biozeron.com). Briefly, raw sequences were processed utilizing the DADA2 pipeline (version 1.30.0) for quality filtering and denoising. Taxonomic classification was executed using the SILVA database (version 138.2). Bioinformatics analysis was performed on the QIIME 2 platform. α-Diversity indices (Shannon index, Chao1 index, and Simpson index) and β-diversity were computed. The relative abundance of taxa was analyzed to assess the effects of experimental interventions. LEfSe analysis was also implemented to discern differentially abundant taxa.

Statistical analysis

The statistical differences in β-diversity among treatment groups were assessed using permutational multivariate analysis of variance (PERMANOVA) in the QIIME 2 platform. A linear discriminant analysis (LDA) score threshold of 6 was applied in the LEfSe analysis to identify differentially abundant taxa in the QIIME 2 platform. For other parameters, statistical analysis was performed using SPSS 26.0 software (IBM-SPSS, Chicago, USA). Prior to one-way analysis of variance (ANOVA), normality was assessed using the Shapiro–Wilk test, and homogeneity of variances was evaluated using Levene's test. Variables not meeting the normality

assumption were logarithmically transformed. Differences among treatment groups were then assessed by one-way ANOVA followed by Duncan's multiple-range test. Spearman correlation analysis was performed to assess the correlation between altered gut microbiota and changes in SCFAs, intestinal integrity, and inflammatory responses. Graphs were generated using GraphPad Prism 8.0 software (GraphPad Software, San Diego, USA). A significance threshold of $P<0.05$ was considered statistically significant, whereas $0.05\leq P<0.10$was interpreted as a trend toward significance.

Results

Isolation, purification and transmission electron microscopy analysis of phages

A lytic phage, designated CP1925, was isolated from sewage samples using the double-layer agar plate method with *Clostridium perfringens* type A strain CP19 as the host bacterium. After purification, the phage formed clear plaques with distinct edges and a uniform distribution on the double-layer agar plates (Fig. 1A). Transmission electron microscopy revealed that phage CP1925 possesses an icosahedral head and a long, slender tail (Fig. 1B). The head was approximately 55 × 45 nm (length × width), with a tail of approximately 60 nm.

Genome information of isolated phages

Phage CP1925 has a genome of 18,159 bp with a GC content of 28.4% (Fig. 4). A total of 22 open reading frames (ORFs) were predicted, distributed in two coding directions. The viral genome was visualized using the R package circlize (Fig. 4). Functional annotation was performed by homologous alignment of the amino acid sequences encoded by the ORFs against the NCBI database. Most of the encoded proteins were hypothetical proteins. Additionally, structural and lysis-related functional genes, such as lysozyme-peptidase and endolysin, were annotated.

Biological characteristics of isolated phages

As shown in Table 2, phage CP1925 lysed only its host strain, CP19, and exhibited no lytic activity against any of the other tested strains, indicating a highly specific host range.

As shown in Fig. 2A, phage titer was highest at an MOI of 10 (2.0×10^8 PFU/mL). Both higher and lower MOI values resulted in decreased titers, suggesting reduced phage proliferation and lower progeny yield. Therefore, the optimal MOI was determined to be 10.

The one-step growth curve (Fig. 2B) showed a latent period of approximately 20 min, followed by a burst phase from 20 to 50 min, during which the titer increased rapidly. After 50 min, the titer entered a plateau phase and remained relatively stable.

As shown in Fig. 3A, at an initial titer of 8.0×10^9 PFU/mL, the phage maintained high lytic activity between pH 3 and 12 after 1 h or 2 h of incubation, with titers remaining above 1.0×10^8 PFU/mL. Phage infectivity decreased markedly at pH 2 and 13, whereas little or no infectivity was detected at the most extreme pH values under the tested conditions.

As shown in Fig. 3B, at an initial titer of 8.0×10^9 PFU/mL, the phage titer remained unchanged after 2 h at 50 °C. At 60 °C for 2 h, the titer decreased but remained above 1.0×10^8 PFU/mL. At 70 °C or higher, the phage became highly sensitive, with a sharp decline in activity, and was completely inactivated within 60 min at 80 °C.

Effects of dietary supplementation with liquid phage CP1925 on growth performance

As shown in Table 3, compared with the CNP group, the HPP group exhibited a significant increase in ADG ($P < 0.05$) and a significant decrease in F/G ($P < 0.05$) during days 8–21. However, during days 22–42 and the overall experimental period (days 8–42), no significant differences in ADFI, ADG, or F/G were observed among groups ($P > 0.05$).

Effects of dietary supplementation with liquid phage CP1925 on jejunal and ileal *Clostridium perfringens* loads

In both the jejunum and ileum (Fig. 5), the TCP group had significantly higher *C. perfringens* loads than the CNP group ($P < 0.05$). Compared with the TCP group, the MCP and HCP groups exhibited significantly lower loads ($P < 0.05$), whereas the LCP group showed no significant difference ($P > 0.05$). No significant difference in C. perfringens DNA abundance was observed between the HPP and CNP groups in either intestinal segment.

Effects of dietary supplementation with liquid phage CP1925 on immune organ indices

Compared with the CNP group (Table 4), the thymus index in the TCP group was significantly decreased ($P < 0.05$). Compared with the TCP group, the thymus index was significantly increased in the MCP and HCP groups ($P < 0.05$), and the bursa of Fabricius index in the MCP group was significantly increased ($P < 0.05$). Moreover, no significant differences in any immune organ indices were observed between the CNP and HPP groups ($P > 0.05$).

Effects of dietary supplementation with liquid phage CP1925 on serum biochemical parameters and immunoglobulins

As presented in Table 5, compared with the TCP group, the MCP and HCP groups showed a significant decrease in the A/G ratio ($P < 0.05$). Phage supplementation did not significantly affect AST, ALT, UA, CREA, TP, ALB, AST/ALT, or Glo in any group ($P > 0.05$). Compared with the CNP group, the TCP group exhibited significantly lower serum IgA and IgG levels ($P < 0.05$). In contrast, compared with the TCP group, the phage-supplemented groups showed significantly increased serum IgA and IgG levels ($P < 0.05$). Additionally, the HPP group had significantly higher serum IgA levels than the CNP group ($P < 0.05$), whereas IgG and IgM levels did not differ

significantly ($P > 0.05$).

Effects of dietary supplementation with liquid phage CP1925 on intestinal inflammatory cytokines

As summarized in Table 6, compared with the CNP group, the TCP group showed significantly increased pro-inflammatory cytokines (IL-1β, IL-6, IL-12, IFN-γ, TNF-α) and decreased anti-inflammatory cytokine IL-10 in both the jejunum and ileum ($P < 0.05$). Compared with the TCP group, phage-supplemented groups exhibited significantly decreased jejunal IL-6 and TNF-α, as well as decreased ileal IL-6, IFN-γ, and TNF-α, while IL-10 levels were significantly increased in both intestinal segments ($P < 0.05$). In the HPP group, jejunal IFN-γ and TNF-α, as well as ileal TNF-α, were significantly decreased, whereas jejunal IL-10, ileal IL-1β was significantly increased relative to the CNP group ($P < 0.05$), with no significant differences in other cytokines.

Effects of dietary supplementation with liquid phage CP1925 on intestinal morphology

Intestinal morphology results are shown in Fig. 6. Compared with the CNP group, the TCP group exhibited significantly decreased VH and CD in both the jejunum and ileum ($P < 0.05$). The VH/CD ratio was significantly increased in the ileum but significantly decreased in the jejunum of the TCP group ($P < 0.05$). Compared with the TCP group, all phage-supplemented groups showed significantly increased jejunal VH ($P < 0.05$), and the HCP group also showed significantly increased ileal VH ($P < 0.05$). The MCP and HCP groups exhibited significantly increased jejunal VH/CD ratio ($P < 0.05$). Relative to the CNP group, the HPP group had reduced VH in both segments; however, these values remained higher than those in the LCP, MCP, and HCP groups. No statistically significant differences were observed for other indicators ($P >0.05$).

Effects of dietary supplementation with liquid phage CP1925 on intestinal permeability parameters

Compared with the CNP group (Fig. 7), the TCP group showed significantly reduced protein expression of Occludin, Claudin-1, and ZO-1 in both the jejunum and ileum ($P < 0.05$). The MCP and HCP groups exhibited significantly increased expression of jejunal Claudin-1 and ileal Occludin compared with the TCP group ($P < 0.05$). Additionally, jejunal Occludin as well as jejunal and ileal ZO-1 were significantly upregulated in the LCP, MCP, and HCP groups compared with the TCP group ($P < 0.05$). Compared with the CNP group, the HPP group showed a significant increase only in jejunal Occludin expression ($P < 0.05$), with no significant differences in the remaining proteins ($P > 0.05$).

Serum permeability results are presented in Table 7. Compared with the CNP group, the TCP group showed significantly elevated serum levels of D-LA, DAO, and LPS ($P < 0.05$). Compared with the TCP group, the LCP, MCP, and HCP groups exhibited significantly reduced serum DAO and LPS levels ($P < 0.05$). In the HPP group, serum LPS was significantly decreased compared with the CNP group, whereas no significant difference was observed in DAO ($P > 0.05$).

Effects of dietary supplementation with liquid phage CP1925 on cecal short-chain fatty acid levels

Compared with the CNP group (Fig. 8), the TCP group showed significantly higher valeric acid levels ($P < 0.05$). Compared with the TCP group, the LCP and MCP groups exhibited significantly increased butyric acid levels ($P < 0.05$). Furthermore, the HPP group had significantly higher butyric acid levels compared with the CNP group ($P < 0.05$), while no significant differences were observed in the other SCFAs ($P > 0.05$).

Effects of dietary supplementation with liquid phage CP1925 on diversity of gut microbiota

As illustrated in Fig. 9, phage supplementation did not significantly alter the α-diversity indices (ACE, Chao1, Shannon, and Simpson) of the cecal microbiota across all treatment groups ($P > 0.05$). For β-diversity assessment based on Unweighted UniFrac distance with statistical testing, Fig. 9E shows clear clustering separations between the TCP and LCP groups, the CNP and HPP groups, and the MCP and HCP groups ($P < 0.05$), indicating distinct microbial community structures.

Effects of dietary supplementation with liquid phage CP1925 on composition of gut microbiota

The microbial composition at the phylum and genus levels (top 10 in relative abundance) across all groups is presented in Fig. 10. Firmicutes and Bacteroidota were the dominant phyla in the cecal microbiota of broilers, with no significant differences in relative abundance at the phylum level among groups ($P > 0.05$). At the genus level, the HPP group exhibited a significantly higher abundance of Blautia compared with the other groups ($P < 0.05$).

LEfSe analysis was subsequently performed to identify bacterial biomarkers with statistical differences among groups, using an LDA score threshold of >6.0 (Fig. 11A). In the TCP group, seven biomarkers were significantly enriched, including *Intestinimonas* (g), uncultured bacterium (s), Erysipelatoclostridiumceae (f), uncultured bacterium (s), Lactobacillus_agilis (s), and *Acetitomaculum* (g). In the CNP group, one uncultured bacterium (s) was enriched. In the MCP group, seven biomarkers were enriched: *Sedimentibacter* (g), Sedimentibacteraceae (f), *Acholeplasma* (g), *B55_F_B_G02* (g), uncultured bacterium (s), *Hydrogenispora* (g), and *Limnochroma* (g). The HCP group showed the most pronounced enrichment, with 41 biomarkers

significantly overrepresented in the cecum. Among these, Lactobacillales (o), Enterococcaceae (f), *Enterococcus* (g), Lachnospiraceae (f), Clostridiales (o), Clostridiaceae (f), Candidatus_Arthromitus_sp_SFB_rat_Yit (s), uncultured bacterium (s), Clostridia (c), and Enterococcus faecium (s) had LDA scores >8.

Correlation analysis between gut microbiota and SCFA, intestinal integrity, and inflammatory responses

Spearman correlation analysis was performed to assess associations between altered microbial genera and parameters of intestinal barrier function, inflammatory responses, and SCFA levels (Fig. 12). For intestinal barrier-related parameters, the abundances of *Akkermansia*, *Bifidobacterium*, *Enterococcus*, and *Odoribacter* were positively correlated with tight junction protein expression (ZO-1 and/or Occludin) in the jejunum or ileum ($P < 0.05$). In contrast, *Candidatus Arthromitus*, *Erysipelatoclostridium*, *Faecalibacterium*, and *Fournierella* showed negative correlations with Claudin-1 and/or Occludin expression ($P < 0.05$). Regarding inflammatory cytokines, positive correlations with pro-inflammatory mediators were identified for several genera: *Faecalibacterium* (with IL-1β, IL-6, IL-12, IFN-γ, TNF-α in both jejunum and ileum), *Agathobacter* (with ileal IL-12, IFN-γ, and IL-1β), *Sellimonas* (with jejunal IL-1β and IL-12), and *Negativibacillus* (with ileal TNF-α). In contrast, negative correlations were found for *Odoribacter* (with ileal IFN-γ and jejunal IL-6) and Bacillus (with jejunal IL-1β and IL-10). For SCFA associations, *Lachnoclostridium* abundance was positively correlated with butyric acid levels ($P < 0.05$), while *Shuttleworthia* showed a positive correlation with valeric acid ($P < 0.05$). In contrast, *Monoglobus* was negatively correlated with isobutyric acid ($P < 0.05$).

Discussion

Phage CP1925 exhibited biological characteristics that supported its evaluation as a targeted intervention against *Clostridium perfringens* [21,22]. Transmission electron microscopy revealed a tailed morphology, and host-range testing demonstrated lytic activity against CP19 but not the other strains examined. The highest propagation titer was achieved at an MOI of 10, with an estimated latent period of approximately 20 min, broadly comparable to those reported for several *C. perfringens* phages [23–25]. CP1925 also retained infectivity following exposure to pH 3–12 and temperatures up to 60 °C under the tested conditions. These properties provide a basis for formulation development, although survival during gastrointestinal transit and feed processing remains formulation-dependent [26,27]. Its narrow host range supports targeted activity against susceptible bacteria and highlights the value of broader isolate screening to establish its potential coverage in poultry production [25,28,29].

Building on this characterization, the animal experiment demonstrated a consistent reduction in intestinal pathogen DNA at the medium and high supplementation doses. Compared with unchallenged controls, challenged birds exhibited greater *C. perfringens* DNA abundance in both the jejunum and ileum, together with gross hemorrhagic changes and histological alterations. These findings support the development of challenge-associated intestinal injury and establish the context for evaluating CP1925 supplementation [30]. Both MCP and HCP reduced pathogen DNA abundance in the two intestinal segments, extending previous evidence that phage supplementation can reduce intestinal *C. perfringens* counts and alleviate NE-associated lesions [15,16,31]. Although qPCR does not distinguish viable bacteria from nonviable cells or extracellular DNA, the concurrence of lower pathogen DNA abundance and improved host indices supports the

441 biological relevance of this response.

442 The host responses further indicate that the effects of CP1925 were not confined to the
443 pathogen endpoint. Challenge reduced the thymus index and serum IgA and IgG concentrations,
444 whereas supplementation improved selected immune organ and humoral indices. The higher
445 thymus indices in MCP and HCP, together with the higher bursa index in MCP, suggest
446 maintenance of immune organ status during challenge. Increased serum IgA and IgG in the
447 challenged supplemented groups provide complementary evidence of altered humoral responses.
448 These changes coincided with lower jejunal IL-6 and TNF-α and higher intestinal IL-10,
449 indicating attenuation of selected inflammatory alterations. Taken together, the results are
450 consistent with modulation of the local inflammatory response alongside improvements in
451 systemic immune indices. The interpretation of these complementary endpoints is consistent with
452 broader approaches to assessing immune and intestinal responses in poultry [32–35].

453 These immune responses were accompanied by changes in mucosal architecture and
454 barrier-related measurements. ZO-1 serves as a scaffolding protein that links the transmembrane
455 protein Occludin to the actin cytoskeleton, providing a structural connection between the
456 junctional complex and the intracellular cytoskeletal network [36]. Improvements in selected villus
457 measurements and jejunal VH/CD ratios suggest better preservation of intestinal structure, while
458 increased Occludin, Claudin-1, and ZO-1 immunostaining in responsive intestinal segments is
459 consistent with maintenance of tight-junction-associated proteins. Similar relationships among
460 mucosal morphology, tight-junction indices, and inflammatory responses have been reported in
461 other interventions against *C. perfringens*-associated intestinal injury [37,38]. In the present study,
462 these tissue-level changes were accompanied by lower serum DAO and LPS, providing

463 complementary evidence of improved barrier-related status [39].

464 The individual barrier indicators nevertheless captured different aspects of the response.
465 Circulating DAO and D-lactate have been evaluated as indirect markers of intestinal barrier
466 dysfunction in chickens, but their responses do not always coincide with those of permeability
467 probes [40]. In the present study, serum D-lactate did not differ significantly among the challenged
468 groups despite reductions in DAO and LPS. This divergence illustrates the value of combining
469 complementary measurements: morphology describes tissue architecture, immunostaining
470 characterizes selected junctional proteins, and circulating markers provide indirect information
471 about mucosal injury and permeability[37–39]. Because *C. perfringens* is Gram-positive and does
472 not produce LPS, lower serum LPS cannot be interpreted as a direct reduction in *C. perfringens*
473 toxin release. It may instead reflect altered exposure to Gram-negative bacterial products or
474 changes in their intestinal passage or systemic clearance. Collectively, these findings support
475 attenuation of selected barrier-related alterations without requiring every indicator to respond in
476 parallel.

477 Examining these outcomes across doses revealed that pathogen DNA and host responses
478 were not fully concordant. MCP and HCP reduced intestinal *C. perfringens* DNA abundance,
479 whereas LCP improved several host indices without a significant reduction in this endpoint. In
480 particular, LCP reduced serum DAO and LPS and increased jejunal villus height and selected
481 tight-junction staining measurements. The low dose thus produced selective host benefits rather
482 than an absence of biological activity. Previous work with phage φCJ22 evaluated graded doses in
483 a *C. perfringens* challenge model and reported dose-associated changes in intestinal bacterial
484 counts and mucosal lesions [16]. A separate study likewise reported reduced intestinal lesion scores

following phage treatment in NE-challenged broilers [41]. Differences in response timing, measurement sensitivity, or the spatial distribution of bacteria may contribute to this pattern. Changes in viable bacterial populations or toxin exposure that were not captured by the DNA measurement are also possible, as conventional qPCR does not necessarily distinguish viable cells from nonviable cells or extracellular DNA [42]. These observations emphasize the value of evaluating supplementation doses across pathogen, tissue, and host-response endpoints.

Within this broader assessment, the medium dose produced benefits across several pathogen, immune, and barrier-related indices and increased cecal butyrate, making it a useful candidate for further dose refinement. The high dose also improved multiple host outcomes but did not consistently provide additional benefits across the measured endpoints. Similarly, a study of a Salmonella-targeting phage in chickens reported differences in antibacterial and microbial responses between low- and high-dose treatments [43]. Although the bacterial target and intervention differed from those in the present study, these findings illustrate the importance of evaluating dose in relation to multiple outcomes. The practical implication is that dose selection should consider the breadth and relevance of the response [44] rather than assume that greater exposure will improve every outcome. The present findings support further evaluation of the medium dose, while a definitive optimal inclusion level remains to be established.

The unchallenged HPP group provided additional insight into how the infection background influences the response to supplementation. Higher serum IgA and jejunal IL-10, lower serum LPS, and increased jejunal Occludin staining indicate that the preparation affected selected host indices even in the absence of experimental infection. These changes occurred alongside higher serum D-lactate and ileal IL-1β and lower villus height in both intestinal segments. In another

chicken model, phage administration in the absence of bacterial challenge was also associated with changes in selected immune responses [45], supporting the value of assessing phage-supplemented birds under both challenged and unchallenged conditions. Other studies have similarly evaluated immune and microbial responses to phage supplementation in chickens without experimental bacterial challenge [46,47]. This mixed response is best interpreted as context-dependent rather than uniformly beneficial or detrimental. Including HPP therefore strengthens the study by distinguishing responses observed during challenge from those occurring in unchallenged birds and by identifying relevant endpoints for subsequent safety assessment.

The microbial results provide an ecological context for these host responses [48,49]. Microbial metabolites can influence epithelial metabolism and the intestinal environment, thereby contributing to resistance against the expansion of potentially pathogenic bacteria, as demonstrated in experimental mouse models [50]. Cecal alpha diversity did not differ significantly among groups, indicating that supplementation did not detectably alter the measured richness and diversity indices. Nevertheless, differences in community composition and LEfSe-associated features suggest responses among selected bacterial populations. Such changes are compatible with indirect effects of targeted antibacterial activity on competition, substrate availability, and the intestinal environment. Their biological interpretation depends on the taxa involved and their relationship to host outcomes, rather than simply on the number of discriminant features. In particular, the larger number of features associated with HCP should not, by itself, be regarded as evidence of either greater efficacy or ecological harm.

Among the taxa examined, *Blautia* relative abundance was highest in HPP. Members of this genus have been associated with microbial fermentation and potential probiotic functions [51,52],

529 making this observation relevant to the response of unchallenged birds. However, the distribution
530 of *Blautia* differed from that of the principal protective responses in challenged groups. Its
531 enrichment should therefore be interpreted as a group-specific microbial response rather than a
532 common explanation for the intestinal benefits of CP1925. Associations involving *Odoribacter*
533 and *Enterococcus* likewise identify candidate relationships with inflammatory and barrier-related
534 indices. Their functional significance is likely to depend on the species and strains present,
535 particularly for *Enterococcus*, which includes both probiotic and opportunistic strains [53]. These
536 findings help prioritize microbial targets for more focused investigation without assigning
537 functions solely from genus-level abundance.

538 The SCFA measurements complement this taxonomic information by providing a metabolic
539 perspective. Beyond its metabolic role, butyrate can support epithelial barrier function through
540 effects on tight-junction regulation. In cultured intestinal epithelial monolayers, sodium butyrate
541 increased Claudin-1 transcription and reduced paracellular permeability, providing direct evidence
542 for a barrier-supporting effect [54]. In the present study, cecal butyrate increased in LCP and MCP
543 relative to TCP, coinciding with improvements in several intestinal indices. Together with
544 evidence that butyrate promotes tight-junction assembly and that SCFAs influence immune and
545 epithelial responses [54–56], these findings provide a biological rationale for considering microbial
546 metabolites as potential contributors to intestinal protection. However, HCP improved several host
547 endpoints without a corresponding significant increase in butyrate. This pattern suggests that the
548 response to CP1925 is unlikely to be explained by a single metabolite or bacterial genus and may
549 involve several interacting processes.

550 Interpreting the microbial and metabolic findings together also requires consideration of

551 intestinal location and metabolite turnover. Cecal SCFA concentrations reflect the balance among
552 production, absorption, utilization, and digesta passage, rather than microbial production alone [57].
553 Moreover, the cecal microbiota and metabolites were measured in a different compartment from
554 the jejunal and ileal host endpoints. These spatial and physiological differences help explain why
555 microbial, metabolic, and tissue responses need not change in parallel [48,49]. The observed
556 associations therefore provide testable hypotheses about the contribution of secondary ecological
557 responses to intestinal protection, rather than establishing a single causal pathway.

558 The distinction between intestinal responses and growth performance is equally important
559 when considering practical application. Despite improvements in selected intestinal indices,
560 CP1925 supplementation did not significantly improve growth relative to the challenged control.
561 The challenge itself did not produce a clear growth reduction relative to CNP, limiting the
562 opportunity to demonstrate recovery of a growth deficit. In addition, the day 8–21 growth interval
563 included an extended pre-challenge period, whereas challenge occurred on days 19–21 and
564 intestinal samples were collected on day 22. The tissue measurements therefore captured relatively
565 acute responses that may not translate directly into measurable growth differences over longer
566 periods.

567 The higher ADG and lower F/G in HPP relative to CNP during days 8–21 further suggest that
568 growth responses depend on both infection background and the period evaluated. These
569 differences were not sustained over days 22–42 or the full supplementation period. Although
570 growth benefits have been reported in other phage studies [15,16], variation in preparation, challenge
571 conditions, and baseline disease severity limits direct comparison with studies in other production
572 settings [58]. Studies of phage–probiotic combinations have also identified additional host benefits

in other infection settings [59], illustrating the potential importance of complementary interventions. Broader work on phage cocktails and poultry applications further supports evaluating formulations according to their bacterial targets and production context [60–62]. For CP1925, the present evidence is strongest for selected intestinal health outcomes and provides a foundation for determining whether these responses translate into production benefits under conditions associated with greater disease pressure.

Several considerations guide the next stage of evaluation. Most intestinal measurements were obtained at a single sampling point, and qPCR did not distinguish viable from nonviable bacteria. Longitudinal measurements, intestinal phage recovery, and viable bacterial or toxin quantification would help clarify the duration and basis of the observed responses. Broader host-range testing and a matched phage-free preparation control would further strengthen practical interpretation. Microbial associations should also be considered in light of the relative nature of sequencing data [63].

Overall, this study provides integrated evidence linking CP1925 supplementation with lower intestinal *C. perfringens* DNA abundance and improvements in selected mucosal, inflammatory, and barrier-related indices. Its particular value lies in comparing graded doses alongside an unchallenged supplementation group, revealing that pathogen, host, and microbial responses are related but not interchangeable. This approach moves beyond antibacterial activity alone and offers a more informative basis for selecting doses and evaluating targeted interventions in poultry. Although sustained production benefits remain to be established, the findings support further development of CP1925 for intestinal health management and identify medium-dose supplementation as a promising candidate for subsequent validation in broiler production.

Conclusions

This study isolated and characterized *Clostridium perfringens* phage CP1925, which possesses a genome of 18,159 bp and a long, non-contractile tail. CP1925 exhibited a narrow host range within the tested bacterial panel, an optimal MOI of 10 for phage propagation, and retained infectivity across pH 3–12 and at temperatures up to 60 °C under the tested conditions. Evaluation of three dietary doses in challenged broilers showed that the effects of CP1925 varied across the measured outcomes, rather than increasing consistently with dose. Medium and high-dose supplementation reduced intestinal *C. perfringens* DNA abundance and improved selected indicators of intestinal morphology, barrier integrity, and immune responses, although no significant improvement in growth performance was observed. The medium dose produced benefits across several intestinal health outcomes and may serve as a candidate dose for further optimization and application studies. Changes in cecal microbiota composition varied among treatment groups, highlighting the importance of considering microbial responses when selecting a supplementation dose. In unchallenged broilers, phage supplementation was associated with changes in selected host and microbial indices, providing an initial basis for evaluating the safety of CP1925 when administered alone. Overall, CP1925 shows potential as a dietary intervention for mitigating NE-associated intestinal injury and supports further investigation of dose selection and safety in broiler production.

Abbreviation	Full term
ADFI	Average daily feed intake
ADG	Average daily gain

Abbreviation	Full term
ALB	Albumin
ALT	Alanine aminotransferase
AST	Aspartate aminotransferase
CD	Crypt depth
CNP	Control group
CREA	Creatinine
D-LA	D-lactate
DAO	Diamine oxidase
F/G	Feed-to-gain ratio
Glo	Globulin
H&E	Hematoxylin and eosin
HCP	High-dose phage group
HPP	Phage-only group
IFN-γ	Interferon-γ
IgA	Immunoglobulin A
IgG	Immunoglobulin G
IgM	Immunoglobulin M
IL-1β	Interleukin-1β
IL-6	Interleukin-6

Abbreviation	Full term
IL-10	Interleukin-10
IL-12	Interleukin-12
LCP	Low-dose phage group
LDA	Linear discriminant analysis
LPS	Lipopolysaccharide
MCP	Medium-dose phage group
MOI	Multiplicity of infection
NE	Necrotic enteritis
ORF	Open reading frame
PBS	Phosphate-buffered saline
PCoA	Principal coordinate analysis
PFU	Plaque forming unit
SCFA	Short-chain fatty acid
TCP	Challenge group
TEM	Transmission electron microscopy
TNF-α	Tumor necrosis factor-α
TP	Total protein
UA	Uric acid
VH	Villus height

Abbreviation	Full term
VH/CD	Villus height-to-crypt depth ratio
ZO-1	Zonula occludens-1

Supplementary Information

Additional file 1. Supplementary figures and table: phylogenetic analysis, predicted ORF functions, and gross intestinal pathological findings..

Acknowledgements

We gratefully acknowledge Phagelux (Nanjing) Biotechnology Co., Ltd. for providing the *Clostridium perfringens* type A strain used in this research.

Authors' contributions

CZ: Conceptualization, Methodology, Investigation, Formal data analysis, Animal trial and data collection, Visualization, Original manuscript writing. JL, KW, FW, MX: Methodology, Animal trial and data collection. YY: Methodology, Manuscript review and editing. KY: Conceptualization, Resources, Supervision, Funding acquisition, Project administration, Original manuscript writing, Manuscript review and editing. All authors have read and agreed to the published version of the manuscript.

Funding

This work was supported by the National Key Research and Development Program of China (2021YFD1300402, 2023YFD1301005) and the Hunan Modern Agricultural Industry Technology System (2024000127).

Data availability

The phage genome sequence has been deposited in NCBI GenBank under accession number PQ261001. The data that support the findings of this study are available from the corresponding author upon reasonable request.

Declarations

Ethics approval and consent to participate

The animal protocol was approved by the Animal Care and Use Committee of the Institute of Subtropical Agriculture, Chinese Academy of Sciences (approval number: 20250819.183).

Consent for publication

Not applicable.

Competing interests

The authors declare no competing interests.

Author details

1 Institute of Subtropical Agriculture, Chinese Academy of Sciences, Changsha, Hunan 410125, China. 2 Chinese Academy of Sciences, Beijing 100039, China. 3 College of Animal Science and Technology, Hunan Agricultural University, Changsha 410128, China.

References

1. Prescott JF, Parreira VR, Gohari IM, Lepp D, Gong J. The pathogenesis of necrotic enteritis in chickens: what we know and what we need to know: a review. Avian Pathol. Abingdon: Taylor & Francis Ltd; 2016;45:288–94. https://doi.org/10.1080/03079457.2016.1139688

2. Rood JI, Adams V, Lacey J, Lyras D, McClane BA, Melville SB, et al. Expansion of the Clostridium perfringens toxin-based typing scheme. Anaerobe. 2018;53:5–10. https://doi.org/10.1016/j.anaerobe.2018.04.011

655 3. Keyburn AL, Boyce JD, Vaz P, Bannam TL, Ford ME, Parker D, et al. NetB, a new toxin that is
656 associated with avian necrotic enteritis caused by Clostridium perfringens. PLoS Pathog. San
657 Francisco: Public Library Science; 2008;4:e26. https://doi.org/10.1371/journal.ppat.0040026

658 4. Collier CT, Hofacre CL, Payne AM, Anderson DB, Kaiser P, Mackie RI, et al. Coccidia-induced
659 mucogenesis promotes the onset of necrotic enteritis by supporting Clostridium perfringens
660 growth. Vet Immunol Immunopathol. Amsterdam: Elsevier; 2008;122:104–15.
661 https://doi.org/10.1016/j.vetimm.2007.10.014

662 5. Lacey JA, Stanley D, Keyburn AL, Ford M, Chen H, Johanesen P, et al. Clostridium
663 perfringens-mediated necrotic enteritis is not influenced by the pre-existing microbiota but is
664 promoted by large changes in the post-challenge microbiota. Vet Microbiol. Amsterdam: Elsevier;
665 2018;227:119–26. https://doi.org/10.1016/j.vetmic.2018.10.022

666 6. Friedman M. Antibiotic-Resistant Bacteria: Prevalence in Food and Inactivation by
667 Food-Compatible Compounds and Plant Extracts. J Agric Food Chem. Washington: Amer
668 Chemical Soc; 2015;63:3805–22. https://doi.org/10.1021/acs.jafc.5b00778

669 7. Cooper IR. A review of current methods using bacteriophages in live animals, food and animal
670 products intended for human consumption. J Microbiol Methods. Amsterdam: Elsevier Science Bv;
671 2016;130:38–47. https://doi.org/10.1016/j.mimet.2016.07.027

672 8. Mohammadi TN, Shen C, Li Y, Zayda MG, Sato J, Masuda Y, et al. Characterization of
673 Clostridium perfringens bacteriophages and their application in chicken meat and milk. Int J Food
674 Microbiol. Amsterdam: Elsevier; 2022;361:109446.

https://doi.org/10.1016/j.ijfoodmicro.2021.109446

9. Xu Y, Liu Y, Liu Y, Pei J, Yao S, Cheng C. Bacteriophage therapy against Enterobacteriaceae. Virol Sin. New York: Springer; 2015;30:11–8. https://doi.org/10.1007/s12250-014-3543-6

10. Wernicki A, Nowaczek A, Urban-Chmiel R. Bacteriophage therapy to combat bacterial infections in poultry. Virol J. London: BMC; 2017;14:179. https://doi.org/10.1186/s12985-017-0849-7

11. Skurnik M, Alkalay-Oren S, Boon M, et al. Nat Rev Method Prim. London: Springernature; 2025;5:10. https://doi.org/10.1038/s43586-025-00387-x

12. Sinclair HA, Lin RCY, Ben Zakour NL, Bollyky PL, Iredell JR. Phage therapy: from basic biology to clinical application. Nat Rev Microbiol. Berlin: Nature Portfolio; 2026; https://doi.org/10.1038/s41579-026-01352-5

13. Hsu BB, Gibson TE, Yeliseyev V, Liu Q, Lyon L, Bry L, et al. Dynamic Modulation of the Gut Microbiota and Metabolome by Bacteriophages in a Mouse Model. Cell Host & Microbe. 2019;25:803-814.e5. https://doi.org/10.1016/j.chom.2019.05.001

14. Miller RW, Skinner J, Sulakvelidze A, Mathis GF, Hofacre CL. Bacteriophage Therapy for Control of Necrotic Enteritis of Broiler Chickens Experimentally Infected with Clostridium perfringens. Avian Dis. Athens: Amer Assoc Avian Pathologists; 2010;54:33–40. https://doi.org/10.1637/8953-060509-Reg.1

15. Muneeb M, Khan EU, Saima null, Suleman M, Awais MM, Ahmad S. Effects of

694 bacteriophage supplementation on performance, gut health and blood biochemistry in broilers
695 challenged with necrotic enteritis. Res Vet Sci. 2025;193:105809.
696 https://doi.org/10.1016/j.rvsc.2025.105809

697 16. Bae D, Lee J-W, Chae J-P, Kim J-W, Eun J-S, Lee K-W, et al. Characterization of a novel
698 bacteriophage φCJ22 and its prophylactic and inhibitory effects on necrotic enteritis and
699 Clostridium perfringens in broilers. Poult Sci. 2021;100:302–13.
700 https://doi.org/10.1016/j.psj.2020.10.019

701 17. Upadhaya SD, Ahn JM, Cho JH, Kim JY, Kang DK, Kim SW, et al. Bacteriophage cocktail
702 supplementation improves growth performance, gut microbiome and production traits in broiler
703 chickens. J Anim Sci Biotechnol. 2021;12:49. https://doi.org/10.1186/s40104-021-00570-6

704 18. Ducatelle R, Goossens E, De Meyer F, Eeckhaut V, Antonissen G, Haesebrouck F, et al.
705 Biomarkers for monitoring intestinal health in poultry: present status and future perspectives. Vet
706 Res. 2018;49:43. https://doi.org/10.1186/s13567-018-0538-6

707 19. Youmans BP, Ajami NJ, Jiang Z-D, Petrosino JF, DuPont HL, Highlander SK. Development
708 and accuracy of quantitative real-time polymerase chain reaction assays for detection and
709 quantification of enterotoxigenic Escherichia coli (ETEC) heat labile and heat stable toxin genes
710 in travelers' diarrhea samples. Am J Trop Med Hyg. 2014;90:124–32.
711 https://doi.org/10.4269/ajtmh.13-0383

712 20. Wang W, Zijlstra RT, Gänzle MG. Identification and quantification of virulence factors of
713 enterotoxigenic Escherichia coli by high-resolution melting curve quantitative PCR. BMC

714 Microbiol. 2017;17:114. https://doi.org/10.1186/s12866-017-1023-5

715 21. Caly DL, D'Inca R, Auclair E, Drider D. Alternatives to Antibiotics to Prevent Necrotic
716 Enteritis in Broiler Chickens: A Microbiologist's Perspective. Front Microbiol. 2015;6:1336.
717 https://doi.org/10.3389/fmicb.2015.01336

718 22. Tian Y, Wu L, Lu R, Bao H, Zhou Y, Pang M, et al. Virulent phage vB_CpeP_HN02 inhibits
719 Clostridium perfringens on the surface of the chicken meat. Int J Food Microbiol.
720 2022;363:109514. https://doi.org/10.1016/j.ijfoodmicro.2021.109514

721 23. Wu LT, Liu BH, Tian Y, Wang J, Bao HD, Zhou Y, et al. Identification and environmental
722 inhibition effect of Clostridium perfringens phage. Acta Vet Zootech Sin. 2022;53(10):3550–3560.
723 doi:[10.11843/j.issn.0366-6964.2022.10.027](https://doi.org/10.11843/j.issn.0366-6964.2022.10.0
724 27). (In Chinese).

725 24. Tian Y. Isolation and characterization of Clostridium perfringens phages and their antibacterial
726 application in raw poultry meat [dissertation]. Zhenjiang: Jiangsu University; 2022.
727 doi:[10.27170/d.cnki.gjsuu.2022.002214](https://doi.org/10.27170/d.cnki.gjsuu.2022.002214). (In
728 Chinese).

729 25. Zhu G, Wang YZ, Zhang MS, Wang XT, Sun J, Wang JC. Isolation, identification and
730 characterization of a Clostridium perfringens phage. Chin J Vet Sci. 2025;45(9):1902–1908.
731 doi:[10.16303/j.cnki.1005-4545.2025.09.11](https://doi.org/10.16303/j.cnki.1005-4545.2025.09.1
732 1). (In Chinese).

733 26. Richards K, Malik DJ. Bacteriophage Encapsulation in pH-Responsive Core-Shell Capsules as

734 an Animal Feed Additive. Viruses-Basel. Basel: MDPI; 2021;13:1131.
735 https://doi.org/10.3390/v13061131

736 27. Chen Y, Ding M, Chen X, Zou T, Liu Y, Chen J, et al. Strategically isolated bacteriophages
737 targeting ETEC K88 (F4) alleviate post-weaning diarrhea in piglets via modulation of gut
738 microbiota and inflammatory responses. J Anim Sci Biotechnol. 2026;17:11.
739 https://doi.org/10.1186/s40104-025-01322-6

740 28. Li MJ, Song ZY, Liu B, Xu ZQ, Liu Y, Wang QL, et al. Isolation, identification and
741 characterization of a virulent phage of Clostridium perfringens. Chin J Vet Sci. 2024;44(8):1691–
742 1697.doi:[10.16303/j.cnki.1005-4545.2024.08.15](https://doi.org/10.16303/j.cnki.1005-4545.2024
743 .08.15). (In Chinese).

744 29. Oromi-Bosch A, Antani JD, Turner PE. Developing Phage Therapy That Overcomes the
745 Evolution of Bacterial Resistance. Annu Rev Virol. Palo Alto: Annual Reviews; 2023;10:503–24.
746 https://doi.org/10.1146/annurev-virology-012423-110530

747 30. Timbermont L, Haesebrouck F, Ducatelle R, Van Immerseel F. Necrotic enteritis in broilers: an
748 updated review on the pathogenesis. Avian Pathol. Abingdon: Taylor & Francis Ltd; 2011;40:341–
749 7. https://doi.org/10.1080/03079457.2011.590967

750 31. Lee H-G, Kim Y-B, Lee S-H, Moon J-O, Chae J-P, Kim Y-J, et al. In Vivo Recovery of
751 Bacteriophages and Their Effects on Clostridium perfringens-Infected Broiler Chickens. Vet Sci.
752 Basel: MDPI; 2022;9:119. https://doi.org/10.3390/vetsci9030119

753 32. Zandi MK, Shirzadi H, Ghasemi HA, Torshizi MAK, Taherpour K, Rahmatnejad E. Protective

754 effects of a multicomponent toxin binder and organic acid blend on feed efficiency, oxidative
755 status, hepatic histology, and jejunal immune-antioxidant responses in broilers co-challenged with
756 aflatoxin B1 and Clostridium perfringens. Poult Sci. Amsterdam: Elsevier; 2026;105:106546.
757 https://doi.org/10.1016/j.psj.2026.106546

758 33. Paul G, Khare V, Gasche C. Inflamed gut mucosa: downstream of interleukin-10. Eur J Clin
759 Invest. Hoboken: Wiley; 2012;42:95–109. https://doi.org/10.1111/j.1365-2362.2011.02552.x

760 34. Qin S, Xiao X, Dai Z, Zhao G, Cui Z, Wu Y, et al. Effects of Bacillus licheniformis on growth
761 performance, immune and antioxidant functions, and intestinal microbiota of broilers. Poult Sci.
762 Amsterdam: Elsevier; 2024;103:103210. https://doi.org/10.1016/j.psj.2023.103210

763 35. Wang H, Ni X, Qing X, Liu L, Lai J, Khalique A, et al. Probiotic Enhanced Intestinal
764 Immunity in Broilers Against Subclinical Necrotic Enteritis. Front Immunol. Lausanne: Frontiers
765 Media Sa; 2017;8:1592. https://doi.org/10.3389/fimmu.2017.01592

766 36. Fanning AS, Jameson BJ, Jesaitis LA, Anderson JM. The tight junction protein ZO-1
767 establishes a link between the transmembrane protein occludin and the actin cytoskeleton. J Biol
768 Chem. 1998;273:29745–53. https://doi.org/10.1074/jbc.273.45.29745

769 37. Du E, Wang W, Gan L, Li Z, Guo S, Guo Y. Effects of thymol and carvacrol supplementation
770 on intestinal integrity and immune responses of broiler chickens challenged with Clostridium
771 perfringens. J Anim Sci Biotechnol. London: BMC; 2016;7:19.
772 https://doi.org/10.1186/s40104-016-0079-7

773 38. Li Z, Wang W, Liu D, Guo Y. Effects of Lactobacillus acidophilus on the growth performance

and intestinal health of broilers challenged with Clostridium perfringens. J Anim Sci Biotechnol. London: Biomed Central Ltd; 2018;9:25. https://doi.org/10.1186/s40104-018-0243-3

39. Zha P, Liu W, Zhou Y, Chen Y. Protective effects of chlorogenic acid on the intestinal barrier of broiler chickens: an immunological stress model study. Poult Sci. Amsterdam: Elsevier; 2024;103:103949. https://doi.org/10.1016/j.psj.2024.103949

40. Gilani S, Howarth GS, Kitessa SM, Tran CD, Forder REA, Hughes RJ. New biomarkers for increased intestinal permeability induced by dextran sodium sulphate and fasting in chickens. J Anim Physiol Anim Nutr (Berl). 2017;101:e237–45. https://doi.org/10.1111/jpn.12596

41. Keerqin C, McGlashan K, Van TTH, Chinivasagam HN, Moore RJ, Choct M, et al. A lytic bacteriophage isolate reduced Clostridium perfringens induced lesions in necrotic enteritis challenged broilers. Front Vet Sci. 2022;9:1058115. https://doi.org/10.3389/fvets.2022.1058115

42. Liu H, Niu YD, Li J, Stanford K, McAllister TA. Rapid and accurate detection of bacteriophage activity against Escherichia coli O157:H7 by propidium monoazide real-time PCR. Biomed Res Int. 2014;2014:319351. https://doi.org/10.1155/2014/319351

43. Wu W-Y, Wang R, An Y-N, Lin Y-Y. Bacteriophage vB_SalS_KY05 controls Salmonella in poultry without disrupting cecal microbiota composition. Vet Q. 2026;46:2617464. https://doi.org/10.1080/01652176.2026.2617464

44. Mohd Shaufi MA, Sieo CC, Chong CW, Tan GH, Omar AR, Ho YW. Multiple factorial analysis of growth performance, gut population, lipid profiles, immune responses, intestinal histomorphology, and relative organ weights of Cobb 500 broilers fed a diet supplemented with

phage cocktail and probiotics. Italian Journal of Animal Science. 2024;23:449–65. https://doi.org/10.1080/1828051X.2024.2321967

45. M P, L G, Ł G, J M, M G, M P, et al. Bacteriophage DNA induces an interrupted immune response during phage therapy in a chicken model. Nature communications [Internet]. Nat Commun; 2024 [cited 2026 Oct 27];15. https://doi.org/10.1038/s41467-024-46555-7

46. Nazir I, Perez D, Vargas SJR, Ur Rehman S, Arora D, Chandra M, et al. Assessing the impact of phage therapy on growth performance, microbiome and phage specific immune response in chickens. Sci Rep. 2026;16:16600. https://doi.org/10.1038/s41598-026-45338-y

47. Sarrami Z, Sedghi M, Mohammadi I, Kim WK, Mahdavi AH. Effects of bacteriophage supplement on the growth performance, microbial population, and PGC-1α and TLR4 gene expressions of broiler chickens. Sci Rep. Nature Publishing Group; 2022;12:14391. https://doi.org/10.1038/s41598-022-18663-1

48. Borda-Molina D, Seifert J, Camarinha-Silva A. Current Perspectives of the Chicken Gastrointestinal Tract and Its Microbiome. Comp Struct Biotechnol J. Amsterdam: Elsevier; 2018;16:131–9. https://doi.org/10.1016/j.csbj.2018.03.002

49. Waite DW, Taylor MW. Exploring the avian gut microbiota: current trends and future directions. Front Microbiol. Lausanne: Frontiers Media Sa; 2015;6:673. https://doi.org/10.3389/fmicb.2015.00673

50. Byndloss MX, Olsan EE, Rivera-Chávez F, Tiffany CR, Cevallos SA, Lokken KL, et al. Microbiota-activated PPAR-γ signaling inhibits dysbiotic Enterobacteriaceae expansion. Science.

New York, N.Y.; 2017;357:570–5. https://doi.org/10.1126/science.aam9949

51. X L, B M, J G, J W, S C, G W, et al. Blautia-a new functional genus with potential probiotic properties? Gut microbes [Internet]. Gut Microbes; 2021 [cited 2026 Oct 17];13. https://doi.org/10.1080/19490976.2021.1875796

52. Gao Z, Li Z, Deng S, Liang S, Nie M, Liu D. Effects of Blautia coccoides CML164 on production performance and meat quality in broiler chickens. Poult Sci. Amsterdam: Elsevier; 2026;105:106452. https://doi.org/10.1016/j.psj.2026.106452

53. Hanchi H, Mottawea W, Sebei K, Hammami R. The Genus Enterococcus: Between Probiotic Potential and Safety Concerns-An Update. Front Microbiol. 2018;9:1791. https://doi.org/10.3389/fmicb.2018.01791

54. Wang H-B, Wang P-Y, Wang X, Wan Y-L, Liu Y-C. Butyrate enhances intestinal epithelial barrier function via up-regulation of tight junction protein Claudin-1 transcription. Dig Dis Sci. 2012;57:3126–35. https://doi.org/10.1007/s10620-012-2259-4

55. Kim CHH. Complex regulatory effects of gut microbial short-chain fatty acids on immune tolerance and autoimmunity. Cell Mol Immunol. Being: Chin Society Immunology; 2023;20:341–50. https://doi.org/10.1038/s41423-023-00987-1

56. Kelly CJ, Zheng L, Campbell EL, Saeedi B, Scholz CC, Bayless AJ, et al. Crosstalk between Microbiota-Derived Short-Chain Fatty Acids and Intestinal Epithelial HIF Augments Tissue Barrier Function. Cell Host Microbe. 2015;17:662–71. https://doi.org/10.1016/j.chom.2015.03.005

834 57. Nakatani M, Inoue R, Tomonaga S, Fukuta K, Tsukahara T. Production, Absorption, and Blood
835 Flow Dynamics of Short-Chain Fatty Acids Produced by Fermentation in Piglet Hindgut during
836 the Suckling-Weaning Period. Nutrients. Basel: MDPI; 2018;10:1220.
837 https://doi.org/10.3390/nu10091220

838 58. Yan L, Hong SM, Kim IH. Effect of bacteriophage supplementation on the growth
839 performance, nutrient digestibility, blood characteristics, and fecal microbial shedding in growing
840 pigs. Asian-Australas J Anim Sci. 2012;25:1451–6. https://doi.org/10.5713/ajas.2012.12253

841 59. Choi Y, Kang A, Seo E, Lee DJ, Park J, Kim Y, et al. Combination of bacteriophage-probiotics
842 alleviates intestinal barrier dysfunction by regulating gut microbiome in a chick model of
843 multidrug-resistant Salmonella infection. J Anim Sci Biotechnol. 2026;17:14.
844 https://doi.org/10.1186/s40104-025-01324-4

845 60. Naghizadeh M, Karimi Torshizi MA, Rahimi S, Dalgaard TS. Synergistic effect of phage
846 therapy using a cocktail rather than a single phage in the control of severe colibacillosis in quails.
847 Poult Sci. 2019;98:653–63. https://doi.org/10.3382/ps/pey414

848 61. Eid S, Tolba HMN, Hamed R, Al-Atfeehy NM. Bacteriophage therapy as an alternative
849 biocontrol against emerging multidrug resistant E. coli in broilers. Saudi J Biol Sci. Amsterdam:
850 Elsevier; 2022;29:3380–9. https://doi.org/10.1016/j.sjbs.2022.02.015

851 62. Thanki AM, Hooton S, Whenham N, Salter MG, Bedford MR, O'Neill HVM, et al. A
852 bacteriophage cocktail delivered in feed significantly reduced Salmonella colonization in
853 challenged broiler chickens. Emerg Microbes Infect. Abingdon: Taylor & Francis Ltd;

2023;12:2217947. https://doi.org/10.1080/22221751.2023.2217947

63. Gloor GB, Macklaim JM, Pawlowsky-Glahn V, Egozcue JJ. Microbiome Datasets Are Compositional: And This Is Not Optional. Front Microbiol. 2017;8:2224. https://doi.org/10.3389/fmicb.2017.02224

Table 1 Diet composition and nutritional levels of experimental broilers

Items	Starter diet (1–21d)	Grower diet (22–42d)
Ingredients, %		
Corn	56.11	60.98
Soybean meal	34.11	27.80
Soybean oil	3.37	4.00
Fish meal	2.56	3.92
Limestone	0.30	0.11
Dicalcium phosphate	2.00	1.76
DL-Methionine	0.25	0.13
Salt	0.30	0.30
Vitamin and mineral premix[1]	1.00	1.00
Total	100.00	100.00
Nutrient level[2]		
Metabolizable energy, MJ/kg	12.54	12.96
Crude protein	21.50	20.00
Lysine	1.25	1.17
Methionine	0.57	0.45
Methionine and cystine	0.91	0.76
Calcium	1.00	0.90
Total phosphorus	0.46	0.40

875 [1]The premix provides the following per kilogram of the diet: VA 12,000 IU, VD_3 2,500 IU, VE

876 20.0 mg, VK_3 3.0 mg, VB_1 3.0 mg, VB_2 8.0 mg, VB_6 7.0 mg, VB_{12} 0.03 mg, pantothenic acid 20.0

877 mg, nicotinic acid 50.0 mg, biotin 0.1 mg, folic acid 1.5 mg, Fe 80 mg, Cu 17.5 mg, I 1.5 mg, Zn

878 105 mg, Mn 124 mg.

879 [2] Calculated value

880

881

882 Table 2 Analysis of the lytic spectrum of phage CP1925

Species	Strain	Source	Lysis activity
Clostridium perfringens	CVCC2032	pig	—
	CP19	chicken	+
	CP23	chicken	—
Salmonella	ATCC14028	chicken	—
	SA926	chicken	—
Escherichia coli	CMCC44103	chicken	—
	ETECK88	pig	—
Enterococcus faecalis	ATCC700802	chicken	—
	Ef1124	chicken	—

883 + = lytic; – = non-lytic

884

885

886

887

888 Table 3 Effects of CP1925 supplementation on broiler growth performance

Items	TCP	CNP	LCP	MCP	HCP	HPP	SEM	*P*-value
8 ~ 21 d								
ADFI, g	56.24	57.27	57.65	58.58	56.60	57.26	0.231	0.513
ADG, g	35.77^{b}	35.00^{b}	34.53^{b}	36.40^{ab}	36.04^{b}	38.24^{a}	0.360	0.020
F/G	1.57^{bc}	1.64^{ab}	1.67^{a}	1.61^{ab}	1.57^{bc}	1.50^{c}	0.0162	0.012
22 ~42 d								
ADFI, g	90.83	92.81	105.32	104.28	89.78	94.62	2.99	0.559
ADG, g	43.75	48.65	53.67	51.52	44.90	47.47	1.28	0.184
F/G	2.08	1.92	1.96	2.02	2.03	2.01	0.0573	0.982
8~ 42 d								
ADFI, g	73.54	75.04	81.49	81.43	73.19	75.94	1.49	0.417
ADG, g	41.85	44.47	47.30	46.76	42.64	45.06	0.746	0.209
F/G	1.76	1.69	1.72	1.74	1.72	1.69	0.0309	0.992

889 Different superscript letters denote statistically significant differences among treatment groups (P

890 < 0.05)

891 Table 4 Effect of CP1925 supplementation on immune organ indexes (g/kg)

Items	TCP	CNP	LCP	MCP	HCP	HPP	SEM	*P*-value
liver	25.08	26.57	23.72	28.5	28.38	26.76	0.625	0.188
spleen	1.10	1.02	0.91	1.15	1.12	0.96	0.041	0.499
thymus	2.39^{b}	3.86^{a}	2.18^{b}	4.50^{a}	3.92^{a}	4.17^{a}	0.214	0.001
bursa	1.71^{bc}	2.00^{abc}	1.56^{c}	2.37^{a}	2.01^{abc}	2.23^{ab}	0.083	0.038

892 Different superscript letters denote statistically significant differences among treatment groups (P

893 < 0.05)

894

895 Table 5 Effects of CP1925 supplementation on serum biochemical parameters and

896 immunoglobulins

Items	TCP	CNP	LCP	MCP	HCP	HPP	SEM	*P*-value
AST, U/L	376.73	455.48	336.53	277.90	298.23	378.50	26.560	0.452
ALT, U/L	5.42	4.78	4.53	4.00	5.10	5.33	0.173	0.145
UA, μmol/L	170.62	166.85	137.20	174.22	207.17	159.83	8.862	0.373
CREA, μmol/L	11.23	13.22	9.97	11.20	11.98	13.02	0.439	0.261
TP, g/L	33.20	31.93	33.43	30.53	29.60	33.40	0.661	0.422
ALB, g/L	10.27	9.62	9.57	8.48	8.30	9.98	0.244	0.096
AST/ALT	70.17	89.85	72.53	71.32	60.20	72.28	3.958	0.450
Glo, g/L	22.93	22.32	23.87	22.05	21.30	23.42	0.446	0.618
A/G	0.47^{a}	0.43^{ab}	0.42^{ab}	0.40^{b}	0.38^{b}	0.42^{ab}	0.008	0.031
IgA, μg/mL	432.41^{c}	534.78^{b}	530.2^{b}	529.43^{b}	546.43^{b}	600.36^{a}	10.66	0.001
IgG,mg/mL	2.34^{b}	2.75^{a}	2.68^{a}	2.58^{a}	2.63^{a}	2.78^{a}	0.0342	0.001
IgM, μg/mL	660.73^{c}	691.99^{abc}	718.7^{ab}	668.25^{c}	$671.96b^{c}$	721.04^{a}	7.168	0.034

897 Different superscript letters denote statistically significant differences among treatment groups (*P*

898 < 0.05)

899

900

901 Table 6 Effects of CP1925 supplementation on intestinal cytokine concentrations (pg/mL protein)

Items	TCP	CNP	LCP	MCP	HCP	HPP	SEM	*P*-value
Jejunum								
IL-1β	28.98^{a}	19.79^{b}	24.71^{ab}	24.23^{ab}	26.85^{a}	25.17^{ab}	0.843	0.036
IL-6	10.42^{a}	4.01^{c}	6.63^{b}	7.34^{b}	6.65^{b}	3.05^{c}	0.433	0.001
IL-10	23.37^{d}	28.92^{c}	37.89^{b}	37.19^{b}	38.41^{b}	45.43^{a}	1.370	0.001
IL-12	8.69^{a}	5.94^{b}	7.41^{ab}	7.27^{ab}	8.06^{a}	7.55^{ab}	0.253	0.036
IFN-γ	15.5^{a}	14.10^{ab}	10.59^{ab}	9.33^{c}	10.45^{ab}	8.92^{c}	0.652	0.006
TNF-α	57.03^{a}	32.04^{bc}	34.14^{b}	32.75^{bc}	29.71^{c}	21.13^{d}	1.982	0.001
Ileum								
IL-1β	24.53^{a}	17.71^{c}	22.86^{ab}	21.00^{b}	20.49^{bc}	21.42^{ab}	0.533	0.002
IL-6	8.76^{a}	5.34^{b}	6.17^{b}	5.5^{b}	2.78^{c}	4.85^{b}	0.398	0.019
IL-10	3.65^{b}	8.37^{a}	9.83^{a}	8.56^{a}	9.26^{a}	9.6^{a}	0.510	0.001
IL-12	3.55^{a}	2.65^{c}	3.29^{ab}	3.01^{bc}	2.93^{bc}	3.07^{bc}	0.075	0.008
IFN-γ	14.47^{a}	8.46^{d}	11.5^{b}	10.54^{b}	10.28^{bc}	8.83^{cd}	0.388	0.001
TNF-α	35.97^{a}	31.68^{b}	27.33^{c}	27.65^{c}	26.46^{c}	21.71^{d}	0.861	0.001

902 Different superscript letters denote statistically significant differences among treatment groups (P
903 < 0.05)

904

905

906

907

908 Table 7 Effects of CP1925 supplementation on serum intestinal barrier markers

Items	TCP	CNP	LCP	MCP	HCP	HPP	SEM	*P*-value
D-LA,μg/L	126.06^{a}	110.61^{b}	124.58^{a}	119.87^{a}	119.72^{a}	120.2^{a}	1.168	0.001
DAO, pg/mL	5.12^{a}	2.42^{c}	3.75^{b}	3.52^{b}	3.81^{b}	2.14^{c}	0.177	0.040
LPS, pg/mL	79.73^{a}	53.24^{c}	64.12^{b}	60.28^{bc}	59.08^{bc}	45.83^{d}	1.879	0.001

Different superscript letters denote statistically significant differences among treatment groups ($P < 0.05$)

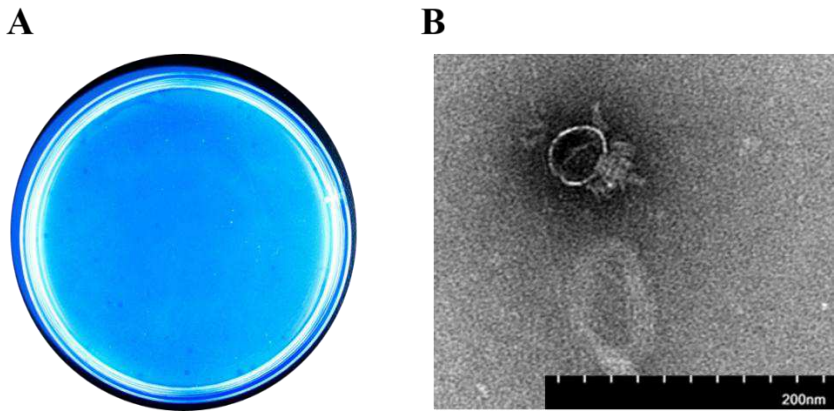


Figure.1 Plaque and electron micrograph of *Clostridium perfringens* bacteriophage CP1925. **A** Plaques of phage CP1925. **B** Transmission electron micrographs of phage CP1925 (scale bar = 200 nm)

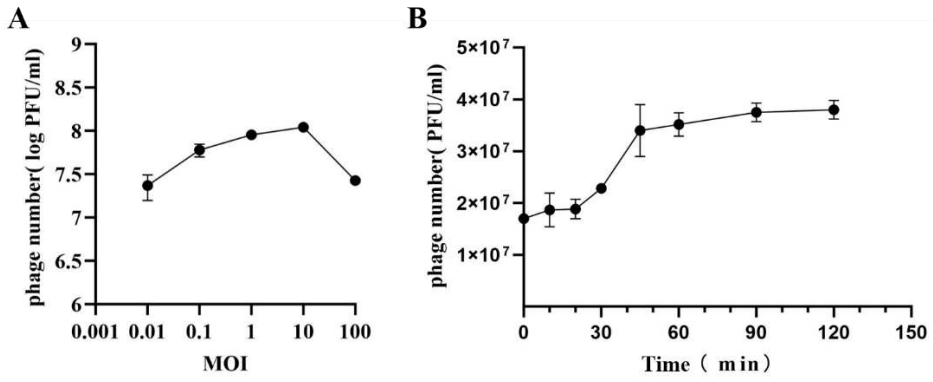


Figure.2 Optimal multiplicity of infection(A) and One-step growth curve(B) of *Clostridium perfringens* phage CP1925 (mean ± SEM; n = 3)

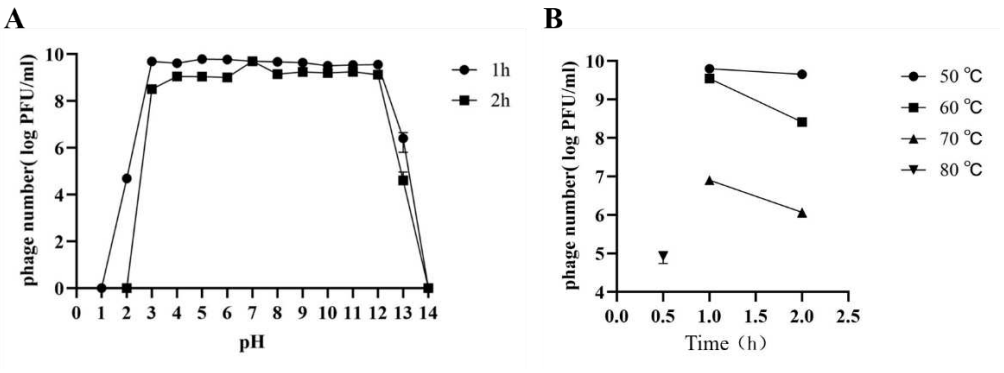


Figure.3 Acid-base stability (A) and thermal stability (B) of *Clostridium perfringens* bacteriophage CP1925 (mean ± SEM; n = 3)

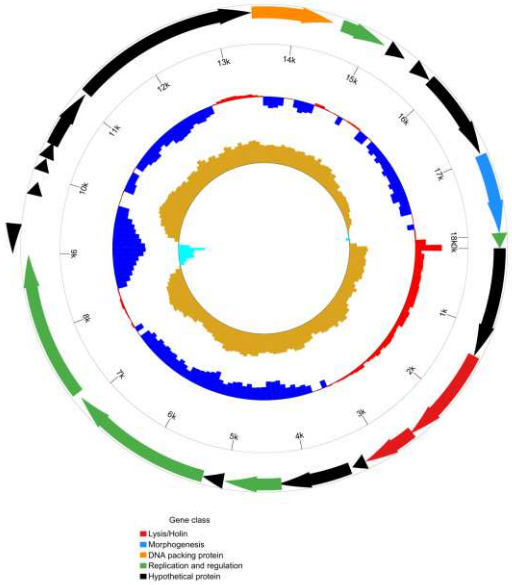
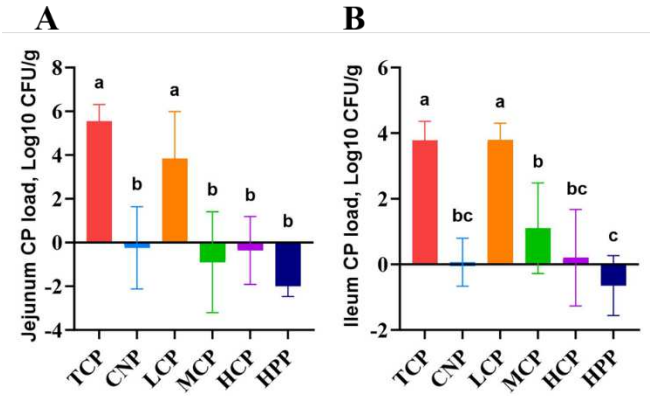


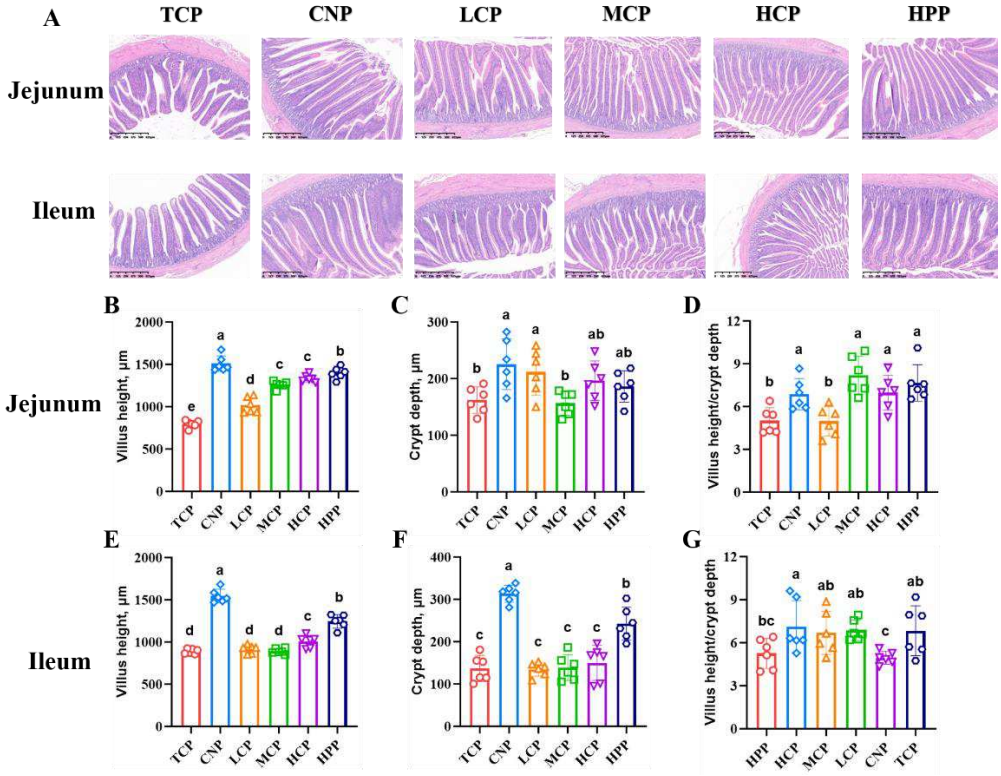
Figure.4 Genome circle map of phage CP1925. Circles were arranged from inside to outside: GC content, genome size markers, and CDS on the positive and negative strands (denoted by distinct colors).



925

926 Figure.5 Jejunal(A) and ileal(B) Clostridium perfringens loads (mean ± SEM; n = 6). Different

927 superscript letters denote statistically significant differences among treatment groups ($P < 0.05$)



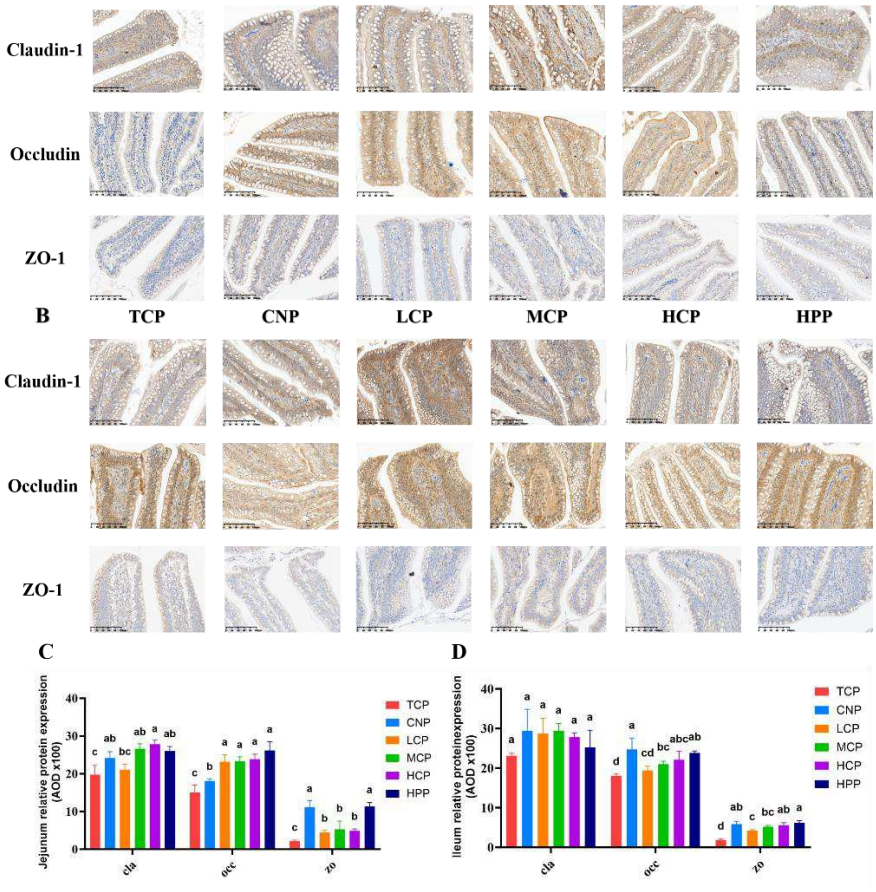
928

929 Figure.6 Effects of CP1925 supplementation on intestinal morphology in broilers (mean ± SEM; n

930 = 6) A H&E images of jejunal and ileal morphology in all groups (scale bar = 125 μm). B–G

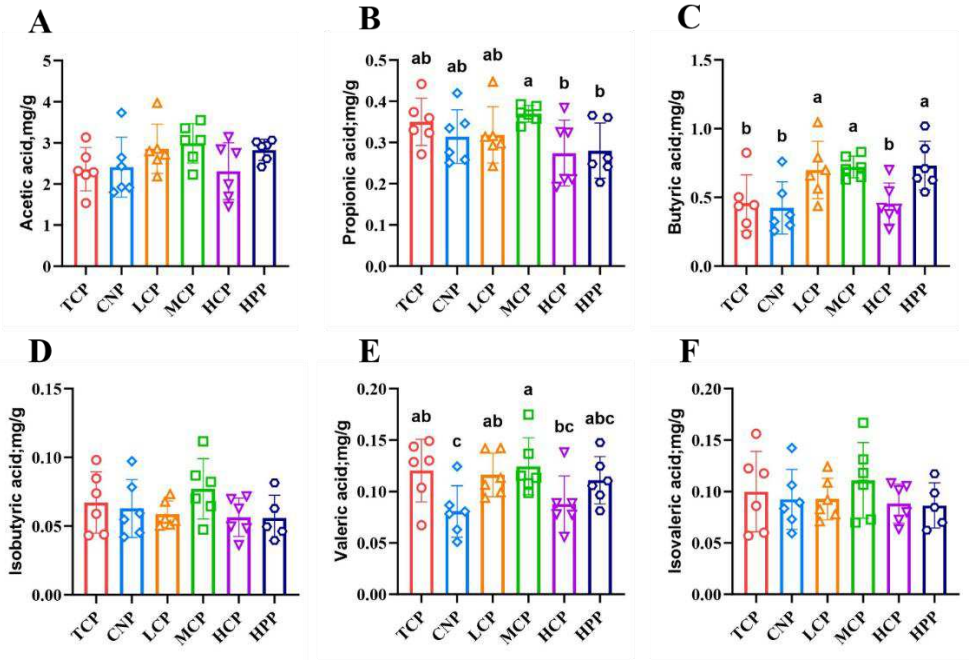
931 Jejunal and ileal villus height, crypt depth, and villus height-to-crypt depth (VH/CD) ratio.

932



933

934 Figure.7 Effect of phage on tight junction proteins in white-feathered broilers. A–B
935 Immunohistochemical analysis of Occludin, Claudin-1, and ZO-1 in the jejunum (A) and ileum
936 (B), respectively (magnification 20×, scale bar = 20 μm). C–D Protein expression levels of
937 Occludin, Claudin-1, and ZO-1 in the jejunum and ileum. Different superscript letters denote
938 statistically significant differences among treatment groups ($P < 0.05$).

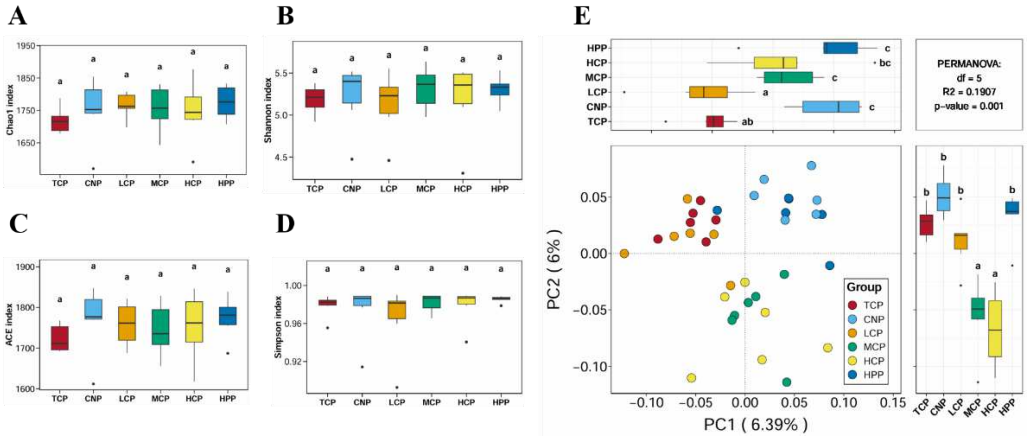


939

940 Figure.8 Cecal short-chain fatty acid levels of white-feathered broilers across the six experimental

941 treatments (mean ± SEM; n = 6). A Acetic acid. B Propionic acid. C Butyric acid. D Isobutyric

942 acid. E Valeric acid. F Isovaleric acid.

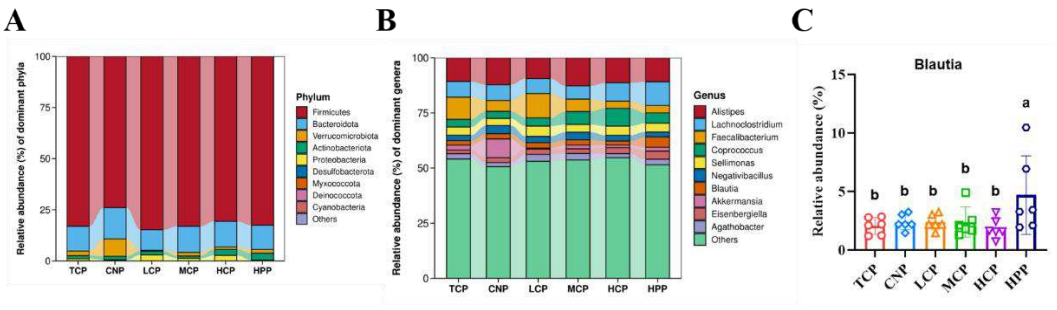


943

944 Figure.9 Analysis of alpha diversity and principal coordinates analysis of cecal microorganisms (n

945 = 6) A Chao 1 index. B Shannon index. C ACE index. D Simpson index. E Principal coordinates

946 analysis (PCoA) plots based on unweighted UniFrac distance metrics .



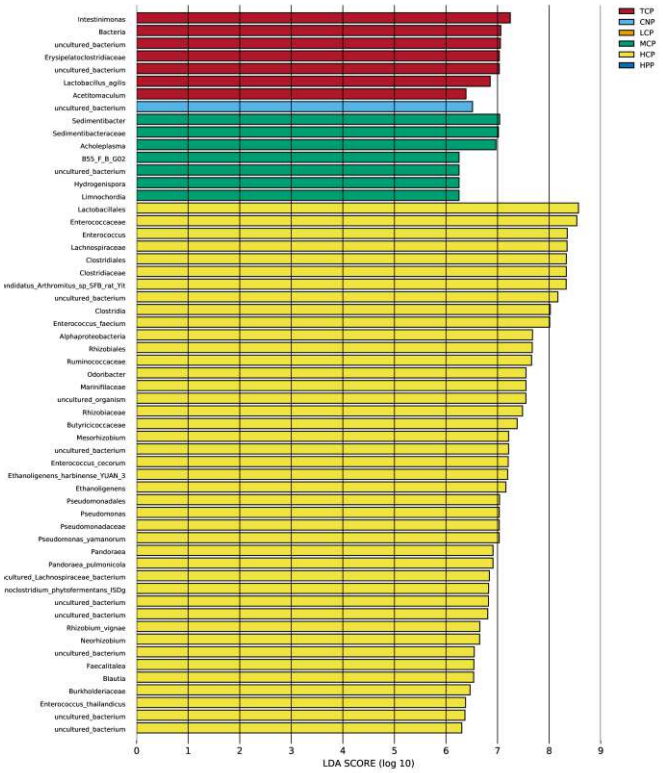
947

948 Figure.10 Cecal microbial composition (n = 6).

949 A–B Relative abundance at the phylum and genus levels. C Relative abundance of Blautia.

950 Different superscript letters denote statistically significant differences among treatment groups (*P*

951 < 0.05).



952

953 Figure.11 LEfSe analysis of the cecal microbial community in broilers (LDA scores > 6.0; n = 6).

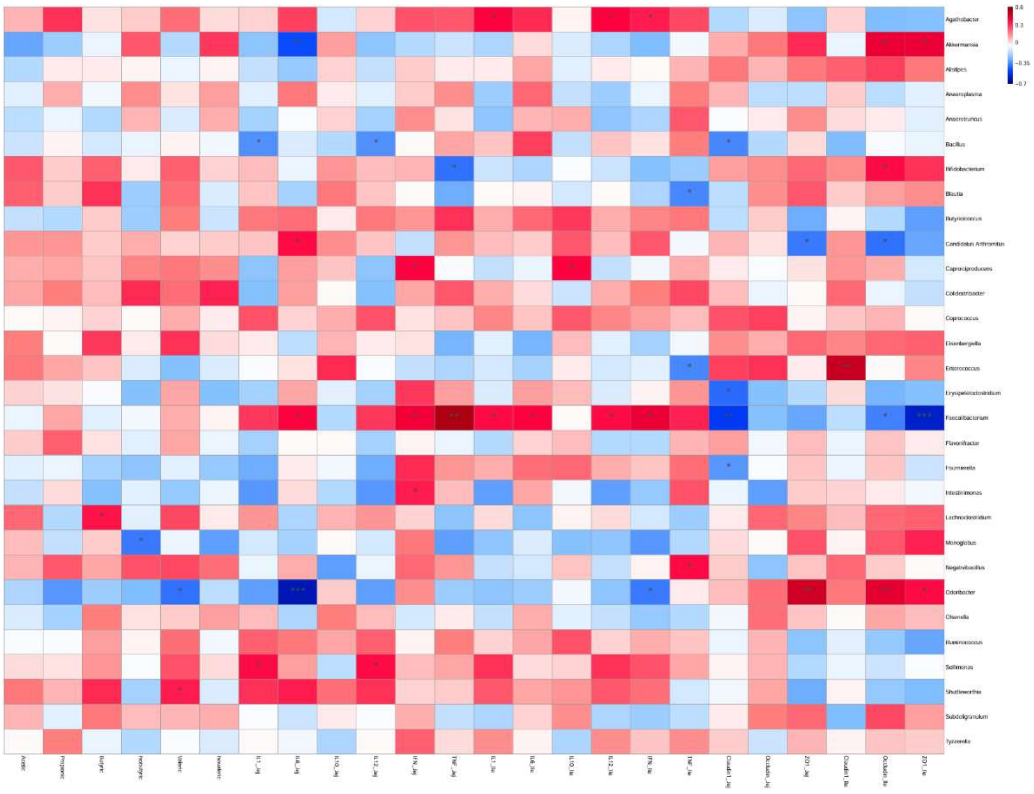


Figure.12 Spearman correlation between gut microbiota and SCFA, barrier, and inflammation. Significant correlations are indicated by *$P < 0.05$, ** $P < 0.01$, *** $P < 0.001$.

Supplementary Files

This is a list of supplementary files associated with this preprint. Click to download.

- phagesupplement1.docx